

# Synchrotron light: From basics to coherence and coherence-related applications

G. MARGARITONDO,<sup>1</sup> Y. HWU<sup>1,2</sup> and G. TROMBA<sup>3</sup>

<sup>1</sup>Institut de Physique Appliquée, Ecole Polytechnique Fédérale de Lausanne, CH-1015 Lausanne, Switzerland

<sup>2</sup>Institute of Physics, Academia Sinica, Nankang, Taipei, Taiwan, ROC

<sup>3</sup>Sincrotrone Trieste SCpA, Trieste, Italy

## Abstract

We show that the basic properties of synchrotron sources can be understood with very simple physics arguments and even simpler mathematical tools. This conclusion includes the fact that such sources provide for the first time in history highly coherent X-rays. In the second part of the article, the basic notions of coherence are presented, followed by a few examples of the first applications of coherent X-rays.

## 1 Introduction

X-rays are the essential tool of an almost endless series of experimental techniques in biology, medical research, physics, chemistry, materials sciences and other disciplines. The most advanced applications rely on the X-ray sources known as "synchrotron sources" [1-3]. The reason is obvious: such sources possess superior qualities with respect to other emitters.

In fact, their qualities progress so rapidly that even experienced users find it difficult to fully exploit them or even just to be aware of them. This is true, in particular, for the high coherence of synchrotron sources, which recently injected a new array of actual and potential techniques into X-ray science[3].

In recent years, simplified empirical treatments were presented[1] that enabled readers to understand the basic properties of synchrotron sources without a complicated mathematical formalism. Our main objective is to extend this simplified approach to coherence properties.

The article begins with a short overview of empirical explanations of basic synchrotron source properties – referring the reader to previously published work[1] for a more detailed discussion. Then, the basic notions of lateral and longitudinal coherence are discussed, with specific reference to the case of synchrotron light. Finally, a few examples are presented of the first practical applications of coherent X-rays.

It should be noted that, consistent with the approach of Ref. 1, no attempt is made to develop a rigorous treatments in detail. Empirical considerations are the focus of our attention, with the objective of intuitively understanding the underlying physics rather than deriving it from a full theoretical treatment. Our hope is to make the coherence of synchrotron sources (as well as other properties) understandable for a non-specialized audience including many of non-physicists – and to enable such an audience to make good use of these superb experimental tools.

## 2 Review of basic synchrotron source properties

In a classical-physics picture, the emission of electromagnetic waves - including X-rays - requires the acceleration of an electric charge. A charge oscillating with a frequency  $\nu$  is in an accelerated motion, thus it emits waves. The emitted waves have many frequencies (and wavelengths), and their spectral peak coincides with the charge oscillation frequency  $\nu$ . A quantum picture does not radically change this description: for example, while emitting a photon during a quantum jump between two atomic levels, an electron does behave like an oscillating charge.

In most emission phenomena the accelerated charges are particles bound to complicated systems – *e.g.*, electrons in atoms, molecules or solids, or ions in solids. Roughly speaking, heavier particles tend to oscillate with lower frequencies (in classical mechanics the fundamental frequency is proportional to  $1/m^{1/2}$ , where  $m$  = mass). Thus, ion oscillations tend to produce infrared light rather whereas electrons mainly produce visible and ultraviolet light as well as X-rays.

The problem in producing X-rays is that the frequencies are much higher than those of visible or ultraviolet light, and difficult to achieve. Synchrotron sources overcome this obstacle by adopting a simple strategy. First, the

emitting electrons are freed from all bounds: rather than being in atoms or solids, they travel as free particles in a vacuum pipe. Second, the electron speed is brought nearly to the speed of light,  $c$ . This causes a series of relativistic effects that shift the emitted frequencies to the X-ray range. Furthermore, relativistic effects produce other desirable effects such as the extreme angular collimation of the emitted X-rays.

The simplest example (Fig. 1a) of this strategy is the so-called[4] inverse Compton scattering: the moving electron bunch collides (1a) with an electromagnetic wave of frequency  $\nu_o$  produced by a laser. The wave is backscattered and its frequency is shifted. The phenomenon can be described as the combination of two steps: first (Fig. 1b), the wave forces the electrons to oscillate in the transverse direction; second (Fig. 1c), the oscillating electrons emit waves in the backscattering direction.

Relativity affects this phenomenon in two ways. First, the electrons “see” the frequency of the wave shifted by the so-called Doppler effect. This is the same type of phenomenon observed, for example, for the sound waves of a train whistle as the train moves towards the observer. Contrary to sound waves, for electromagnetic waves the Doppler shift it is a relativistic phenomenon and must be treated as such.

The relativistic Doppler theory shows that the moving electrons “see” the incoming wave frequency shifted from  $\nu_o$  to  $2\gamma\nu_o$ . Here the “gamma-factor”  $\gamma$  characterizes the relativistic properties of the moving electron, and is defined as the electron energy  $mc^2$  divided by its Einstein’s rest energy,  $m_o c^2$ :

$$\gamma = mc^2/m_o c^2. \quad (1)$$

On the other hand, the backscattered waves are observed from the point of view of the laboratory as waves emitted by moving sources (the electrons). Thus, their frequency is again Doppler-shifted by a factor  $2\gamma$ , leading to a very large overall shift:

$$\nu = 4\gamma^2\nu_o. \quad (2)$$

In summary, the inverse Compton scattering can be used to convert a low-frequency wave (*e.g.*, the emission of an infrared laser) into high-frequency X-rays. As a practical example, consider a primary photon beam of photon energy  $h\nu_o = 0.1$  eV. Suppose that the electron energy  $mc^2 = 50$  MeV. Since the electron rest energy  $m_o c^2 \approx 0,5$  MeV, we have  $\gamma \approx 100$  and  $4\gamma^2 \approx 4 \times 10^4$ . Thus, the backscattered photon energy is  $h\nu \approx 4\gamma h\nu_o \approx 4 \times 10^4 \times 0.1 = 4 \times 10^3$  eV – indeed, a frequency in the X-ray range.

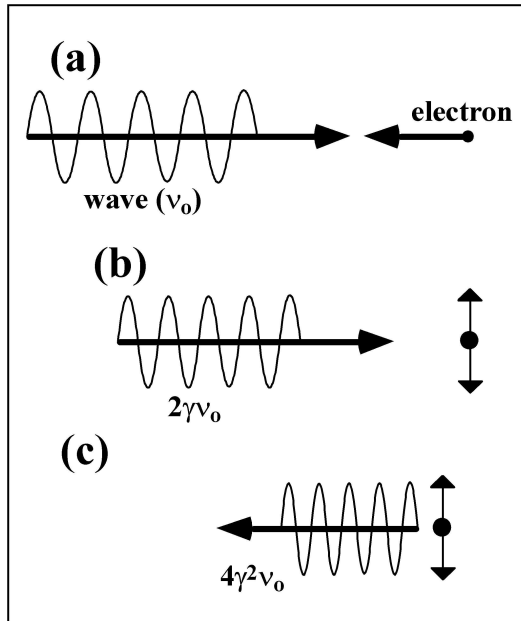


Figure 1: Schematic explanation of a way to exploit relativity in order to produce X-rays: inverse Compton scattering (Ref. 4). The phenomenon can be analyzed as the effect of a wave of frequency  $\nu_0$  which interacts (a) with an electron moving at relativistic speed. Seen by the moving electron, the wave frequency (b) is Doppler-shifted to  $\approx 2\gamma\nu_0$ . The wave forces the electron to oscillate and to emit waves. Seen from the laboratory frame (c), the frequency of these backscattered waves is again Doppler shifted, becoming  $\approx 2\gamma^2\nu_0$ .

Compton backscattering has indeed been used (by Frank Carrol *et al.* and other authors – see Ref. 4) for the production of X-rays. However, its applications are still limited with respect to those of synchrotron sources, which are based on a slightly different strategy. Instead of using a primary wave, they simulate its effects by using a stationary periodic series of magnets (Fig. 2a). Technology enables us to build excellent magnet systems of this type with a period  $L$  of the order of 1 cm. Relativity *de facto* transforms this macroscopic period into the microscopic wavelength of an X-ray beam.

Once again we must “see” the period magnet array from the point of view of the moving electrons (Fig. 2b). Relativity says that the periodic magnetic field becomes the combination of a periodic magnetic field and of a perpendicular electric field of the same frequency. In other words, it “looks” from the electron point of view as a full electromagnetic wave with

its oscillating electric and magnetic components.

What is the frequency of this wave? The answer is: the speed of light divided by the wavelength. One could imagine that the wavelength is simply given by  $L$ , the magnet array period. But this is not true: the moving electrons see the length  $L$  decreased by a factor  $\approx 1/\gamma$  because of the relativistic effect known as “Lorentz contraction”. Thus, the wavelength becomes  $L/\gamma$ , and the frequency becomes  $\gamma c/L$ .

The moving electrons backscatter the equivalent wave created by the magnet array, thus producing the electromagnetic waves known as “synchrotron radiation”. Note, however, that the frequency of these waves is not  $c\gamma/L$ . Seen from the laboratory point of view (Fig. 2c), this frequency is in fact modified by the Doppler shift, becoming:

$$\nu \approx 2\gamma^2 c\gamma/L \approx 2\gamma^2 c/L. \quad (3)$$

Note the similarities between Eqs. 2 and 3: in both cases the  $\gamma^2$  factor reflects the combination of two relativistic effects, which greatly increases the emitted frequency bringing it to values in the X-ray range.

Here is a practical example for Eq. 3: an electron beam of energy  $mc^2 = 2 \text{ GeV}$  and therefore with  $\gamma \approx 4 \times 10^3$ . A magnet array of period  $L = 1 \text{ cm} = 10^{-2} \text{ m}$  gives electromagnetic waves of frequency  $\nu \approx 10^{18} \text{ s}^{-1}$ . The corresponding photon energy  $h\nu \approx 6.6 \times 10^{-16} \text{ joule} \approx 4 \times 10^3 \text{ eV}$  is well into the X-ray range. One can reach the same conclusion by noting that the frequency of Eq. 3 corresponds to a wavelength  $\lambda = c/\nu = L/(2\gamma^2)$ . Thus, the double relativistic effect shrinks by a factor  $2\gamma^2$  the macroscopic magnet period  $L = 10^{-2} \text{ m}$ , producing a microscopic wavelength  $\lambda \approx 3 \times 10^{-10} \text{ m} = 3 \text{ \AA}$ , typical of X-rays.

Periodic magnet arrays - known as “undulators” or “wigglers” - are widely used in modern synchrotron sources. They are part of a much larger system known as a “synchrotron light facility”.

A typical synchrotron facility includes a storage ring, which is a closed-loop vacuum pipe within which electrons circulate at nearly the speed of light. Along this pipe there are several straight section where wigglers or undulators are inserted to produce synchrotron radiation – which is then collected and utilized by suitable “beamlines”. With good vacuum, the stored electrons can circulate for very long periods of time, exceeding in some cases one day.

The electrons are first produced and pre-accelerated in a suitable injection system, and then injected and stored in the storage ring. There they are kept circulating in closed orbits by a sophisticated system of magnets.

The basic components of the magnet system are “bending magnets”, *i.e.*, dipole magnets which bend the trajectory to keep the electrons in closed orbits. As the electrons lose energy by emitting synchrotron radiation, their circulation in the ring requires an equivalent injection of energy at each turn. This is done with a radiofrequency cavity, providing the right electric field each time an electron bunch enters it.

The bending action of bending magnets is of course an acceleration, which also produces the emission of synchrotron radiation. Once again the frequency peak of the emitted wave is shifted towards the X-ray domain by a combination of two relativistic effects. One of them is again the Doppler effect – which shifts the frequency by a factor  $\approx 2\gamma$ . As to the other effect, classical physics suggests that the peak frequency should correspond to the angular speed of the electrons along the bent trajectory, divided by  $2\pi$ . In fact, a circulating charge in a circular orbit looks like a charge oscillating with that frequency when seen from the side.

The classical-physics treatment of the motion of an electron subject to

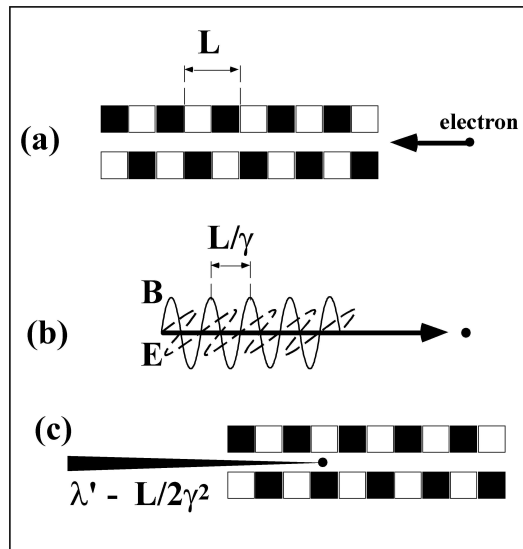


Figure 2: Undulator emission (Refs. 1-3): in this case, the incoming wave is replaced by a static periodic magnet field, produced by an undulator (a). The static field, seen by the electrons moving at relativistic speed, looks like an electromagnetic wave (b), whose wavelength is the period  $L$  of the magnet array shrunk to  $L/\gamma$  by the relativistic Lorentz contraction. The electron oscillating under the influence of the undulator emit synchrotron light. Seen from the laboratory frame (c), the wavelength of this emission is again Doppler-shifted, becoming  $\approx L/2\gamma^2$ .

the Lorentz force of a constant B-field (cyclotron motion) shows that the angular speed is simply  $eB/m_o$ . Taking relativity into account, the force magnitude changes by a factor of  $\gamma$  and so does the angular speed, becoming  $\gamma eB/m_o$ . The corresponding emitted frequency peak is  $\gamma eB/(2\pi m_o)$  in the electron frame. After Doppler-shifting, the laboratory-frame spectral peak is:

$$\nu = 2\gamma^2 eB/(2\pi m_o), \quad (4)$$

which again includes the characteristic  $\gamma^2$  factor.

Bending-magnet emission was the first type of synchrotron light used for practical applications, since it was automatically emitted by electron accelerators. Even today, many productive beamlines are still fed by bending magnet sources rather than by undulators or wigglers.

## 2.1 Bending magnets, undulators, wigglers: What do they have in common?

The answer is: many things, two of which are most important. The first is that all these sources emit “a lot of waves”. Consider for example bending magnets. The emitted power flux, according to classical physics, is proportional to the square of the acceleration. The acceleration is given by the product of the electron speed ( $\approx c$ ) times the angular speed  $\gamma eB/m_o$ , therefore its square is proportional to  $\gamma^2 B^2$ . Considering the high values of  $\gamma$  in typical storage rings, this tremendously increases the emitted flux with respect to the classical case. Similar considerations lead to corresponding conclusions for undulators.

The second common property of all sources is the very high angular collimation of the emission. This is the result of the high speed of the source (the electron), which combines with that of the emitted wave to “project forward” and therefore collimate the emission. A similar effect is present, for example, for sound waves emitted by a moving car or by a moving train.

For electromagnetic waves, however, the effects must be treated taking into account relativity and in particular the invariance of the speed of light. The key result can be derived with a simple argument. Consider a ray of synchrotron light, emitted in a given direction. In the reference frame of the moving electron (Fig. 3). this is the direction of the velocity vector of the light beam. The velocity component in the “forward” direction is  $(dx/dt)$ , and that in the transverse direction is  $(dy/dt)$ . The angle of the emission direction is determined by the ratio  $(dx/dt)/(dy/dt)$ .

How do these components change when seen in the laboratory frame? The relativistic (Lorentz) transformation  $(x,y,t) \rightarrow (x',y',t')$  includes a factor  $\gamma$  for the transformed time interval  $dt'$  and for the “forward”  $dx'$ , but not for the “transverse”  $dy'$ . Therefore, the ratio  $(dx'/dt')/(dy'/dt')$  decreases by a factor  $\approx 1/\gamma$  with respect to  $(dx/dt)/(dy/dt)$ . Since  $1/\gamma$  is small, this implies extreme collimation: the angular spread of synchrotron light does not exceed  $\approx 1/\gamma$ . For undulators, one can show[2] that the angular spread is further reduced by a factor  $\approx 1/N^{1/2}$ , where  $N$  is the number of periods in the magnet array.

## 2.2 Bending magnets, undulators, wigglers: What are the differences?

The primary difference is the spectral width. *i.e.*, the width of the emitted band of frequencies around the peak value of Eq. 3 or Eq. 4. Consider, first, a bending magnet source and a small-area detector (Fig. 4a). Because of the angular collimation, the emitted synchrotron light of an electron looks like a very narrow “torchlight”. At each passage of the electron, the detector “sees” a rapid pulse of synchrotron radiation. On the other hand, a rapid pulse of light corresponds to a broad spectrum of frequency (Fourier) components, therefore the emitted spectral peak will be very wide on the frequency axis.

The duration of the pulse,  $\Delta t$ , can be easily calculated[1] and used to derive the corresponding frequency bandwidth  $\Delta\nu \approx 2\pi/\Delta t$ . The value of this bandwidth is equal to that of the peak frequency (Eq. 4), thus for a bending magnet:

$$\Delta\nu/\nu \approx 1. \quad (5)$$

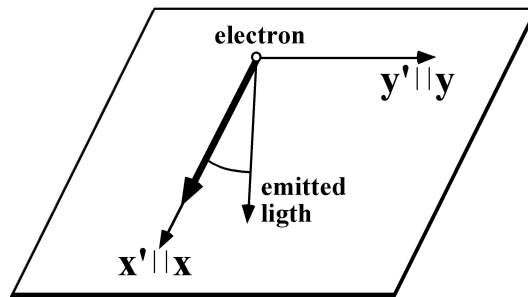


Figure 3: Reference frames used to treat the Lorentz transformation and to explain the collimation of synchrotron light.

This is a pretty wide bandwidth, which in the standard log-log plot of the emitted peak looks even broader (see again Fig. 4a). From this broad spectrum, much narrower bands can be filtered by suitable monochromators along each beamline, as required for specific applications.

Consider now an undulator (Fig. 4b): if the magnet-induced transverse “undulations” are gentle, the emitted light cone of synchrotron light never leaves the detector area. Thus, the detected pulse is long rather than short, and the bandwidth is narrow. In fact, the pulse duration is not anymore the key factor for the bandwidth, which is determined instead by the diffraction-grating-like monochromatizing effect of the magnet array. As for all diffraction gratings, the relative bandwidth is simply determined by the number of periods:

$$\Delta\nu/\nu \approx 1/N. \quad (6)$$

The undulator emission, therefore, is a narrow peak. How can the position of this peak be modified as required for specific applications? The solution to this problem can be understood with very simple considerations.

Equation 3, which defines the undulator peak emission, was derived using  $2\gamma$  as the Doppler shift factor. In turn,  $\gamma$  is determined by the energy of the moving electrons, and therefore by their speed. However, the undulator-induced oscillations of the electron trajectory effectively reduce the “forward” speed by adding a transverse component. Therefore, the “effective” (forward)  $\gamma$ -value decreases, and according to Eq. 3 this changes the emitted peak.

The transverse speed increases (and the forward speed decreases) as the undulator B-field increases. Therefore, one can tune the emitted peak by changing B, typically by changing the distance separating the magnet poles.

There is an upper limit, however, in changing the B-field strength. When the electron undulations become too large, the emitted light cone does not continuously illuminate the detector – see Fig. 4c. Instead of a long pulse, the detector “sees” a series of short pulses, corresponding once again to a broad bandwidth as for bending magnets. The magnet array in this case is not called an “undulator” but a “wiggler”. The wiggler emission is equivalent to that of a series of bending magnets combined in series.

### 2.3 Other properties

Our present empirical discussion will not deal with all the properties of synchrotron sources. This is not because simple explanations are not possible. On the contrary, virtually all synchrotron light properties can be

understood[1] with simple treatments primarily based on elementary electromagnetism and relativistic effects – similar to what we have seen above. We present here a couple of additional examples.

The first case concerns the polarization of the emitted waves – see Fig. 5. For comparison, imagine a charge oscillating along an antenna. The charge emits linearly polarized waves in the direction perpendicular to the antenna – *i.e.*, waves whose electric field is in the direction of the antenna. Imagine now to observe a circulating electron from the side of a storage ring (or an electron in an undulator from the forward axis of the magnet array). In both cases, the observed electron motion is an oscillation, reminiscent of a charge oscillating along an antenna.

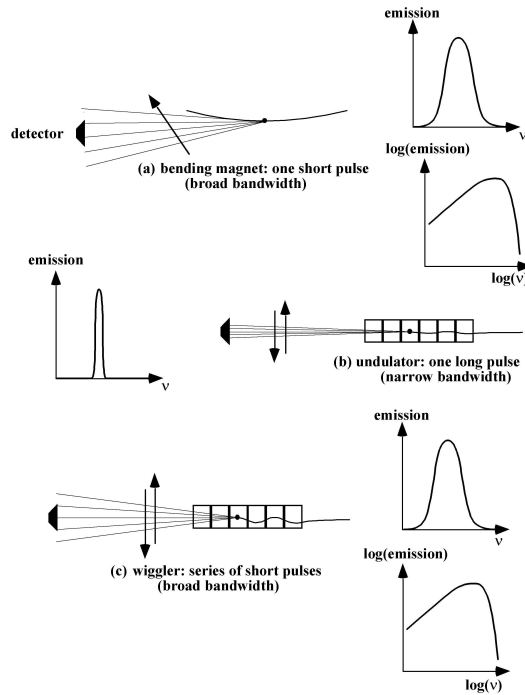


Figure 4: Three different sources of synchrotron light: (a) for a bending magnet, a passing electron with its narrow emission cone creates one short pulse at the detector. Thus, the spectral emission occurs over a large band of frequencies; the standard log-log plot enhances the impression of a large bandwidth. (b) For an undulator (small transverse oscillations), the emission cone continues to illuminate the detector for a long period of time, and the emitted spectral peak is narrow. (c) For a wiggler, the transverse undulations are large and the detector “sees” a series of short pulses, again producing a large bandwidth.

We can thus understand why the emission is linearly polarized in the plane of the ring. But the conclusion cannot be generalized. For example, by moving our viewpoint slightly out of the ring plane, we see the electrons moving along an elliptic-like trajectory (Fig. 5a) – and we understand why the off-plane emission is elliptically polarized.

Elliptical polarization is quite important for many interesting applications. However, because of its collimation the emitted light decreases quite rapidly as we leave the plane of the ring. Thus, off-axis emission is not an ideal solution to the problem of producing elliptically polarized synchrotron light.

On the other hand, an undulator can be designed to produce electron undulations not only in one transverse direction, but along an elliptic spiral. Such a device can produce a very intense and highly polarized beam with elliptic polarization, which are extremely useful for specialized applications.

Finally, consider (Fig. 6) the time structure of the emitted radiation. We have seen that each electron produces a pulse of light each time it passes in front of a bending-magnet beamline. But this is not the most important factor in the actual time structure of the emitted light. We must also consider the fact that the circulating electrons are bunched together. A light pulse is thus produced at the beamline during the passage of the entire bunch rather than of a single electron. The actual time structure consists of such light pulses separated by “dark” periods. This time structure finds interesting applications in time-resolved experiments.

Why are the circulating electrons bunched together? The answer is simple: we have seen that the radiofrequency cavity must restore the electron energy by timing its electric field to the passage of electrons after each turn around the ring. This is only possible by grouping the electrons in one or

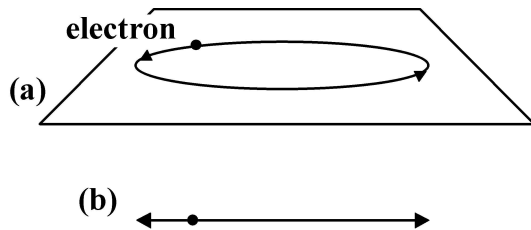


Figure 5: Elementary analysis of the polarization of synchrotron light. (a) A circulating electron seen from outside the plane of the orbit appears as moving along an elliptical trajectory. The corresponding emission is elliptically polarized (circular plus linear). (b) Seen from the plane of the ring, the emission appears linearly polarized.

several bunches.

### 3 A Special parameter: The brightness or brilliance

The quality of a synchrotron source must be characterized with special parameters. To some extent, the choice of the parameter depends on the specific application: certain source characteristics are important for some applications but irrelevant or even negative for others.

One parameter, however, can be used for the majority of the applications: the “brightness” or “brilliance” [1-3]. As schematically explained in Fig. 7, this parameter is the combination of the emitted flux  $F$  and of two kinds of geometric characteristics: the source size ( $S_y$  and  $S_z$  in the transverse  $y$  and  $z$  directions) and the angular spreads ( $\Delta\theta_y$  and  $\Delta\theta_z$ ) of the emitted beam:

$$\text{brightness or brilliance} = \text{constant} \propto F / (S_y \Delta\theta_y S_z \Delta\theta_z). \quad (7)$$

Therefore, a source can be made brighter by increasing the flux, by decreasing the size or by enhancing the angular collimation.

Why is brightness important? On one hand, the desirability of a higher flux is evident: more flux means more signal for the experiments. But why combining (Eq. 7) the flux with geometric factors?

The answer is provided by fundamental optics. The brightness of a photon beam cannot be changed by an (ideal, *i.e.*, lossless) optical system. This implies that to focus a beam of fixed flux (as required for many applications),

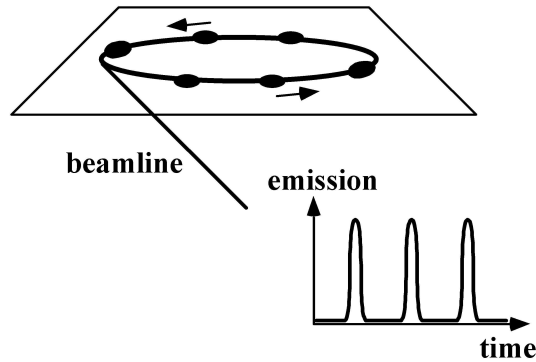


Figure 6: The actual time structure of synchrotron light is determined by the “bunching” of the electrons circulating around the storage ring.

one must accept an increase in angular spread. But this often requires expensive or unavailable large-size optical devices. By and large, a beam is much more easily handled if it comes from a high-brightness source.

The comparison between a light bulb and a laser is - quite literally - very illuminating: the bulb may emit more light, but the laser is more effective because it concentrates its emission in a small area and in a narrow angular range, thereby achieving higher brightness.

How can the brightness of a synchrotron source be increased? In the first place, by increasing the flux. The average flux emitted by each single circulating electron is fixed by the electron motion parameters (as discussed above). One could, however, increase the number of circulating electrons, *i.e.*, the stored current in the ring. Unfortunately, the improvements in that sense practically saturated at  $\approx 1$  ampère in the 1980's.

The other possible way to increase the brightness (Eq. 7) is to improve the source geometry. This requires a better control of the motion of circulating electrons. Each individual electron follows its own trajectory, which slightly deviates from the "reference" ideal trajectory. The cross section of the bunch of all trajectories determines the size of the synchrotron radiation source. Likewise, the small angular deviations of each electron trajectory from the "reference" trajectory contribute to the overall angular spread of the emitted synchrotron radiation, in addition to the "natural" spread  $\approx 1/\gamma$ .

Spectacular improvements in the electron motion control led in the past twenty years[2,3] to increases in the source brightness by many orders of magnitude. How far can we go? The answer to this important question

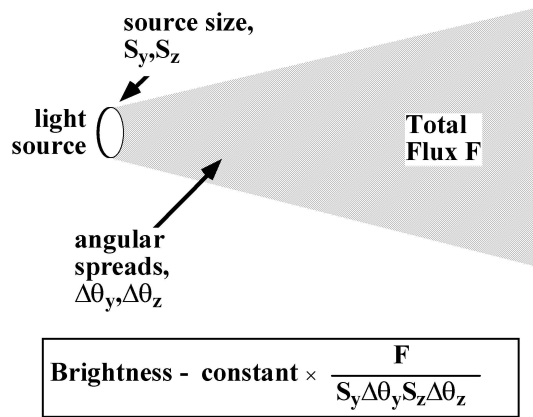


Figure 7: Simplified definition of brightness (or brilliance).

is very simple: no improvement will be able to overcome the “diffraction limit” (see later), *i.e.*, to bring the  $S_y\Delta\theta_y$  or  $S_z\Delta\theta_z$  products in Eq. 7 below a minimum value linked to the wavelength  $\lambda$ .

## 4 What makes a synchrotron source “Coherent”?

The efforts to improve the source geometry thereby improving the brightness yielded a very important byproduct: coherence. The most recent synchrotron sources are “fully coherent” down to wavelengths in the ultraviolet and soft-X-ray range – and quite coherent for shorter wavelengths[3]. This is a landmark event: for the first time, more than one century after Röntgen’s discovery, we can utilize coherent X-rays! This means opening up a huge array of novel techniques, many of which are already used at longer wavelengths.

Before discussing its applications, we must understand what coherence is and why synchrotron sources are becoming highly coherent. Once again, we will emphasize empirical aspects rather than mathematical formalism.

A “wave” is characterized by its potential capability to produce wave-specific phenomena like interference and diffraction. However, such phenomena are rarely seen in everyday life even if we are continuously surrounded by waves like light or sound. “Coherence” is what makes a wave capable to produce *observable* interference and diffraction effects.

In order to focus our discussion, consider the diffraction produced by a circular slits of diameter  $d$  (Fig. 8a). Suppose that the wave source is a point source that emits a single wavelength  $\lambda$  (*i.e.*, a single frequency  $\nu = c/\lambda$ ). Then, the diffraction manifest itself with a series of circular fringes at the detector.

We can therefore conclude that a point-like single-wavelength (monochromatic) source is a coherent source. But what happens if the source is no longer monochromatic, or no longer point-like, or both? The fringes will be blurred and, beyond a certain point, no longer visible. This point marks the difference between coherent and non-coherent sources.

### 4.1 Lateral coherence – the “Diffraction limit”

We consider first a finite source size, modelled (Fig. 8b) by two point sources at a distance  $S_z$  from each other. Each point source produces its own fringe pattern, and the two patterns are superimposed at the detector. The centers of the two patterns are at an angular distance of  $S_z/D$  radians from each other ( $D = \text{source-pinhole distance}$ ).

The elementary theory of diffraction tells us that the angular distance between two adjacent fringes is  $\approx \lambda/d$  radians. If this value is substantially larger than  $S_z/D$ , then the superposition of the two patterns gives a somewhat blurred but still clearly visible set of fringes. Thus, the first condition for source coherence - known as “lateral coherence” or “spatial coherence” - is  $S_z/D < \lambda/d$ , or  $S_z(d/D) < \lambda$ .

Note that  $(d/D) \approx \Omega_z$ , where  $\Omega_z$  is the “illumination angle” of each of the two slits. Thus, the condition for spatial coherence can be written:

$$S_z \Omega_z < \lambda. \quad (8)$$

This equation implies that while reducing the source size  $S_z$  we improve not only the source brightness but also the spatial coherence.

The source angular collimation is also important for spatial coherence:

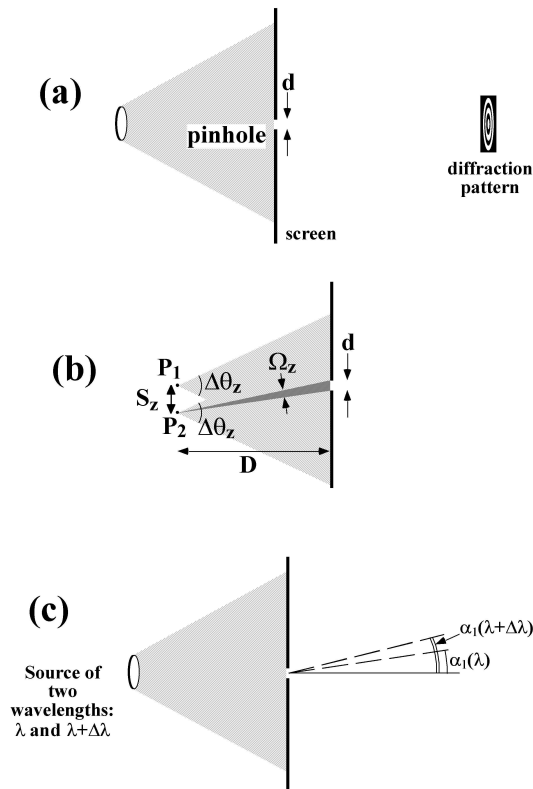


Figure 8: Simplified analysis of spatial coherence. (a) Diffraction by a circular slit, whose analysis is used to discuss: (b) lateral coherence, and (c) longitudinal coherence.

let us see why. Suppose (see Fig. 8b again) that each one of the two point source has an angular divergence  $\Delta\theta_z$ . Only a portion of this angular emission can be used to produce a detectable fringe pattern. According to Eq. 8, this portion is  $\lambda/S_z$ . This implies that of the entire emission over the angular range  $\Delta\theta_z$  only a fraction  $(\lambda/S_z)/\Delta\theta_z = \lambda/(S_z\Delta\theta_z)$  can be used to produce coherence-requiring phenomena.

By increasing the source collimation, *i.e.*, by decreasing  $\Delta\theta_z$ , one increases this fraction. A similar conclusion is valid for the  $y$ -direction, leading to the definition of the “coherent power” of the source – the fraction of the emitted power that can be used to produce coherence-requiring phenomena:

$$\text{Coherent power} \approx [\lambda/(S_y\Delta\theta_y)][\lambda/(S_z\Delta\theta_z)] = \lambda^2/(S_y\Delta\theta_y S_z\Delta\theta_z). \quad (9)$$

Equation 9 enables us to generalize the previous conclusion about the correlation between increases in brightness and increases in spatial coherence. In fact, when the brightness is increased (Eq. 7) by decreasing one or more of the source geometry parameters  $S_y$ ,  $\Delta\theta_y$ ,  $S_z$ ,  $\Delta\theta_z$ , then the coherent power is also enhanced.

Also note that the coherent power increases with the square of the wavelength. Reaching high spatial coherence is thus more difficult for X-rays than for visible light.

How much spatial coherence can one obtain? Equation 9 suggests that if  $S_y\Delta\theta_y$  (or  $S_z\Delta\theta_z$ ) equals the wavelength, the source is “fully coherent” along  $y$  (or  $z$ ). This is the so-called “diffraction limit”, and it can be easily understood in the following way.

Take a large-size, angularly divergent source and try to convert it into a small-size, collimated source. This is possible, for example, by using a shield with a pinhole placed at a large distance from the original source. The approach is rather inefficient, since the shield blocks most of the emission – but it does succeed in improving the source geometry.

However, the pinhole produces diffraction, which contributes to the angular spread. If the pinhole size is  $S_y$  in the  $y$ -direction, then the diffraction-caused angular spread  $\Delta\theta_y$  is  $\approx \lambda/S_y$ . This implies that the product  $S_y\Delta\theta_y$  (or  $S_z\Delta\theta_z$ ) cannot become smaller than  $\lambda$ .

Note that this is not a technological limit but a fundamental optics property: no source can have better geometric characteristics than the diffraction limit. This limit corresponds both to the maximum brightness for a given flux and to full spatial coherence.

What is the present situation? Sources of the class of ELETTRA, BESSY-II and ALS are fully coherent down to wavelengths of the order

of 1,000 Å. The Swiss Light Source will move this limit down to  $\approx 100$  Å. Within this spectral range, the Swiss light source will thus have unsurpassable geometric characteristics: not even an “X-ray laser” can do better.

## 4.2 Longitudinal coherence

This is the coherence condition related to the non-monochromaticity of the source, *i.e.*, to its bandwidth  $\Delta\lambda$ . To simplify the analysis, consider a point source emitting only two wavelengths,  $\lambda$  and  $\lambda + \Delta\lambda$  – see Fig. 8c. Each wavelength produces a fringe pattern. Specifically, the first-order fringe for  $\lambda$  occurs at the angle  $\lambda/d$  radians, and that for  $\lambda + \Delta\lambda$  at  $(\lambda + \Delta\lambda)/d$  radians.

These fringes are difficult to observe in the superposition pattern if they are too much shifted from each other. On the contrary, if  $\lambda/d \approx (\lambda + \Delta\lambda)/d$  then they are blurred but visible. This implies  $\Delta\lambda \ll \lambda$ , or:

$$\Delta\lambda/\lambda \ll 1. \quad (10)$$

Equation 22 expresses a condition of “longitudinal coherence” or “time coherence”. Depending on the specific phenomenon, the actual condition can be more or less stringent – and quite forgiving in some cases, only requiring  $\Delta\lambda/\lambda$  to be slightly smaller than 1.

In some applications of longitudinal coherence, what matters is the so-called “coherence length”,  $L_c$ . This notion can be understood by noting that two waves of wavelengths  $\lambda$  and  $\lambda + \Delta\lambda$ , which happen to be in phase at a certain point in space, will become out of phase beyond this point. Specifically, they will be totally out of phase (*i.e.*, the maximum on one wave coincides with the minimum of the other) after a distance  $L_c$  such that  $L_c/\lambda - L_c/(\lambda + \Delta\lambda) = 1/2$ , which for a small  $\Delta\lambda$  gives  $L_c\Delta\lambda/\lambda^2 \approx 1/2$ , or:

$$L_c \approx \lambda^2/(2\Delta\lambda). \quad (11)$$

In other words, the coherence length characterizes the distance over which the phase difference between the two waves becomes significantly large.

Is synchrotron radiation longitudinally coherent, *i.e.*, is its bandwidth  $\Delta\lambda$  sufficiently narrow? The answer depends on the specific application. In some cases, the bandwidth of an undulator (Eq. 6, implying  $\Delta\lambda/\lambda \approx 1/N$ ), or even that of a bending magnet (Eq. 5, implying  $\Delta\lambda/\lambda \approx 1$ ) are sufficient. In other cases the emission must be filtered by a suitable monochromator to further decrease  $\Delta\lambda$ .

In general, the monochromatization is easier when the source is bright. Therefore, brightness is also somewhat connected to the longitudinal coherence, although in a much less direct way than to spatial coherence.

## 5 How can we use coherent X-rays?

Coherence is a recent development for X-rays, therefore its applications are still quite limited. The potential, however, is tremendous, ranging from unconventional radiology to microscopic-scale metrology and to X-ray holography.

Our objective is not to present a review of the present and potential applications, but to illustrate with a few practical examples the possible future impact of coherence on X-rays research. We selected the oldest and most important use of X-rays: radiology.

### 5.1 Refractive-index radiology

Radiology is important because it can image “hidden things” in medical, biological and materials science specimens. It does so by exploiting the low absorption coefficient of X-rays. The contrast in radiological images originates from differences in the absorption coefficient. As the absorption is weak, the differences are also weak. This creates serious difficulties in very important applications like mammography for breast cancer screening.

What else, however, could one use to achieve contrast in radiology? The answer is found in a more complete description of the interaction between X-rays and materials. Consider a simple case: a monochromatic plane wave in vacuum along the x.-direction:

$$A \exp(ikx) \exp(-i\nu t/2\pi) .$$

Its interaction with a material is described by the *complex* refractive index,  $n = n_R + in_I$ . In the material,  $k$  is replaced by  $nk$ , and the wave becomes:

$$A \exp(-n_I kx) \exp(in_R kx) \exp(-i\nu t/2\pi) .$$

The  $\exp(-n_I kx)$  factor gives the attenuation due to absorption. The  $\exp(in_R kx)$  factor is an oscillating wave and describes the effects of the classic (real) *refractive index*. Radiology, since Röntgen’s discovery, has been only based on absorption. But could one use instead effects related to the (real part of the) refractive index, described by the  $\exp(in_R kx)$  factor?

This is a very attractive idea: the differences from material to material in the real part of the refractive index, although still small for X-rays, are more pronounced than the absorption differences. Furthermore, the real

part of the refractive index and its differences between materials decrease less rapidly with the wavelength than absorption.

Apparently, we implemented radiology in an ineffective way for over one century! There are, of course, good reasons for this “mistake”: using refractive-index effects requires superior-quality X-ray sources, which were not available until quite recently.

This point can be easily understood. One can exploit for radiology different effects related to the (real part of the) refractive index: diffraction, refraction, interference etc. All such effects, however, require a collimated beam of X-rays, and in some cases a highly coherent beam. In the past, such beams could be obtained from conventional X-rays sources by using pinholes. But the price was the waste of most of the emission – and a flux too low for most practical applications.

The picture dramatically changed when synchrotron sources arrived with their superior collimation and coherence. The results, as we will see shortly, are quite spectacular.

## 5.2 Refraction and diffraction effects

The difference between conventional, absorption-based radiology and refractive-index-based radiology can be quite striking indeed – see for example the direct comparison of Fig. 9. What are the causes of this difference? To explain this point, sophisticated image-formation theories are presented in the literature[5]. Here, following again our empirical approach, we will illustrate basic mechanisms by using simple modelling.

### 5.2.1 Edge Diffraction Contrast

Consider the case of Fig. 10a: the edges between vacuum and a partially opaque object illuminated by a monochromatic point-source. The absorption by the object contributes to the image formation on the detector by shading the projected area. In addition, because of the coherence of the source, one can observe the phenomenon known as “Fresnel edge diffraction” (or edge interference). This produces sharp bright-dark fringes which enhance the visibility of the object edges[5,6].

The theory of this effect for fully opaque objects[6] is a classic problem in optics, discussed by in any textbook under standard approximations. Calling  $z$  the transverse coordinate (Fig. 10b),  $z = 0$  the detector coordinate,  $-z_o$  the edge coordinate, and  $r_o$  and  $r_d$  the source and detector distances from the plan of the object, the detected intensity is expressed[6] in terms of sine

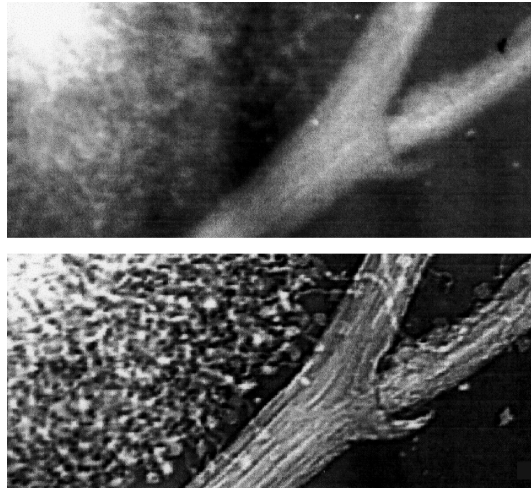


Figure 9: Direct comparison of two radiological images of a mimosa flower. Top: conventional (absorption) image; bottom: coherence-enhanced image. Data from Arfelli *et al.*, Ref. 5.

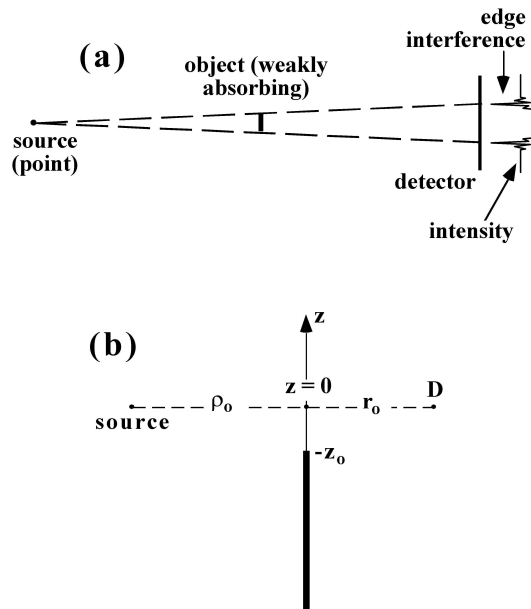


Figure 10: Simplified analysis of the edge enhancement mechanism by Fresnel edge diffraction, based on a coherent source.

and cosine “Fresnel integrals”:

$$Intensity(-u_o) = constant \infty [C(\infty) - C(-u_o)]^2 + [S(\infty) - S(-u_o)]^2, \quad (12)$$

where  $u$  is the standard reduced variable for Fresnel integrals:

$$u = [2(\rho_o + r_o)/\rho_o r_o \lambda]^{1/2} z, \quad (13)$$

and  $-u_o$  is its value for  $z = -z_o$ .

A standard analysis[6] (often based on the “Cornu spiral” method) shows that Eq. 12 gives indeed a series of bright-dark fringes as  $z_o$  and therefore  $u_o$  increase.

In the case of X-rays, the object is not opaque but partially transparent. Furthermore, its (real) refractive index changes the phase of the waves which travel through it. This case can be treated as a simple extension of the previous analysis. Under reasonable approximations (see Ref. 6 ), the result corresponding to Eq. 12 is:

$$Intensity(-u_o) = constant \infty \{1 + \phi[C(-u_o) - S(-u_o)]\}, \quad (14)$$

which again gives a series of bright-dark fringes, with the first occurring for  $u_o \approx 0.7$  and  $u_o \approx -0.7$ .

What are the conditions for observing such fringes? First of all, the resolution of the detector must be sufficient to separate a bright fringe from the adjacent dark fringes. Note, from Eq. 13, that for a given value of  $u_o$  the actual coordinate  $z_o$  changes as the detector distance  $r_o$  changes – and so does the  $z$ -distance between bright and dark fringes. Specifically, this distance increases as  $r_o$  increases. Given a detector with a certain resolution, one can thus try to detect the fringes by placing it far enough from the object.

This is indeed how the image formation in Fig. 9 was changed from the “absorption” mode to the “edge diffraction” mode. Alternatively, one can use a detector with high enough resolution[6] to detect the fringes even when placed close to the object.

The second condition concerns longitudinal coherence: if the source emits a wide bandwidth  $\Delta\lambda$ , then the fringes may become too blurred and no longer visible. We have seen that the  $u_o$ -distance between the first bright fringe and the adjacent dark fringe is  $\approx 0.7 - (-0.7) = 1.4$ . The corresponding “real”  $z$ -distance is (Eq. 13):

$$\delta z \approx [\rho_o r_o \lambda / 2(\rho_o + r_o)]^{1/2} \infty 1.4.$$

A bandwidth  $\Delta\lambda$ , *i.e.*, a “blurring” of the wavelength would “blur”  $\delta z$  by  $\Delta(\delta z)$ , in such a way that  $\Delta(\delta z)/\delta z \approx \Delta\lambda/2\lambda$ . But the fringes are

still distinguishable if  $\Delta(\delta z)/\delta z < 1$ , thus the condition for longitudinal coherence is:

$$\Delta\lambda/2\lambda < 1, \quad (15)$$

which is a rather forgiving version of Eq. 10 – and, for most synchrotron sources, does not even require a monochromator.

The third condition concerns spatial coherence. More specifically, what matters in this case is primarily the source size (although the collimation is helpful in concentrating a high flux on the object). Consider a source of finite size  $S_z$  instead of a point source. This would blur the fringe pattern by  $\approx(r_o/\rho_o)S_z$ . The fringes are still visible if  $(r_o/\rho_o)S_z$  does not exceed the bright-dark distance  $\delta z \approx [\rho_o r_o \lambda / 2(\rho_o + r_o)]^{1/2} \approx 1.4$ :

$$(r_o/\rho_o)S_z < [\rho_o r_o \lambda / 2(\rho_o + r_o)]^{1/2} \approx 1.4. \quad (16)$$

As a typical example, take  $\rho_o = 20$  m,  $r_o = 2$  m and  $\lambda = 1$  Å. Eq. 16 approximately gives  $S_z < 140$   $\mu$ m, which is again a rather forgiving condition. In fact, diffraction-enhanced radiology could have been implemented with synchrotron sources of the 1980's generation – or even with conventional X-rays sources equipped with pinholes. However, the high flux of modern synchrotrons sharply decreases the time required to take an image, and makes it possible to perform real-time experiments.

Note that the condition of Eq. 16 becomes progressively less stringent as the distance ratio  $(\rho_o/r_o)$  increases. This, however, is in conflict with the requirement to increase the object-detector distance to compensate the limited detector resolution – and makes even more desirable to use high-resolution detectors.

### 5.2.2 Refraction contrast

The model of Fig. 10 assumes that the edge is infinitely sharp, which is not true in most cases. Finite-width edges can produce another type of edge-enhancement in radiological images. This is still related to the real refractive index, but is due to refraction rather than to edge diffraction.

A simple model[7] is presented in Fig. 11: a tapered edge between vacuum and an object which partially absorbs but also refracts an X-ray beam. The (weak) absorption does produce some contrast. However, the edge visibility is strongly enhanced by the refraction in the edge region, which produces a bright pseudo-fringe plus a dark pseudo-fringe.

No longitudinal coherence at all is required for this refraction mechanism of edge enhancement. As to other conditions, even a simple analysis encounters significant difficulties. In fact, no general conditions can be derived for this case, since the enhancement mechanism depends on the specific shape of each edge. Qualitatively considerations, however, still yield interesting results.

Call  $a$  the distance between the centers of the dark and illuminated pseudo-fringes on the detector and  $b$  the width of each pseudo-fringe. The distance  $a$  is determined by the width of the tapered edge, thus it is a morphological characteristic of the object. On the other hand, the fringe width is given by  $b \approx r_o \alpha$ , where  $\alpha$  is the refraction-induced angular deviation of the X-ray beam (which in turn depends on the edge slope and on the real part of the object refractive index) – thus it increases with the object-detector distance  $r_o$ .

When  $b$  becomes too big, *i.e.*, when no longer  $b < a$ , it becomes difficult to separate the dark fringe and the illuminated fringe. Therefore, contrary to what happens for the diffraction-based edge enhancement, the refraction-based enhancement becomes less visible when  $r_o$  increases. On the other hand, when  $r_o$  is too small the limited detector resolution makes it impossible to observe the refraction-induced edge enhancement as it does for the diffraction-induced edge enhancement.

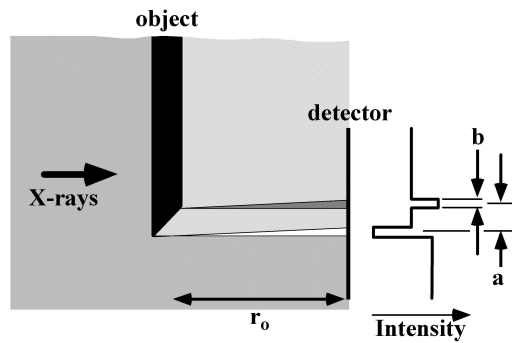


Figure 11: Simplified analysis of the enhancement of a tapered edge by a refraction mechanism, again based on a coherent source.

Qualitatively speaking, therefore, the refraction-based edge enhancement is visible only within a certain interval of object-detector distances. The same conclusion is valid if the edge, rather than separating the object from vacuum, is between two different specimen areas with different refractive index.

These qualitative conclusions can be transformed into quantitative results under reasonable assumptions – see Ref. 7. The interesting point is that one can play with the geometry of the experiment to enhance either the edge diffraction mechanism or the refraction mechanism, and match the requirements of specific applications.

### 5.3 Some recent examples

Figures 12 and 13 show two recent, spectacular examples of coherence-enhanced radiographic images[13]. Their quality requires no comment. Note that very small details can be observed, opening up many new opportunities in microradiology.

Figure 14 directly illustrates the interplay between diffraction-enhanced and refraction-enhanced coherent radiology[7]. We see on the right the characteristic series of diffraction fringes for each edge. On the left, only a pair of fringes are seen for each edge. The transition from one regime to the other (center) is accomplished, as mentioned above, by changing the geometry, *i.e.*, by changing the distance  $r_o$  between source and detector. The transition can be quantitatively justified[7] with the simple models of the previous two sections.

Finally, we would like to mention that coherence-based radiology was recently extended to live specimens[8]. Spectacular real-time images of different organs in live animals were obtained with high lateral resolution and excellent contrast. These positive tests indicate that the extension to human patients is not too far away.

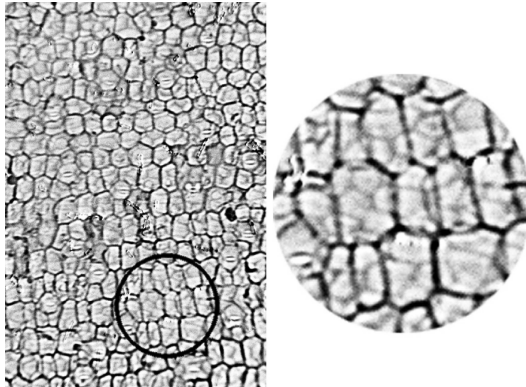


Figure 12: A recent example (Hwu, Je *et al.*, Ref. 13) of coherence-enhanced radiological image, showing the microstructure of a leaf.

## 6 Future sources

Can X-ray sources be further improved? The answer is a qualified “yes”. There exists some flexibility for additional improvements of storage-ring sources, but also the possibility of using entirely different sources: the “free electron lasers”.

As we see already mentioned (Eq. 7), the brightness of an X-ray source can be improved by either increasing the flux  $F$  or by improving the geometric parameters. In a storage ring, each circulating electron emits synchrotron light stochastically, acting as an independent source. The total flux can thus be increased by increasing the number of circulating electrons, *i.e.*, the total current of the electron beam.

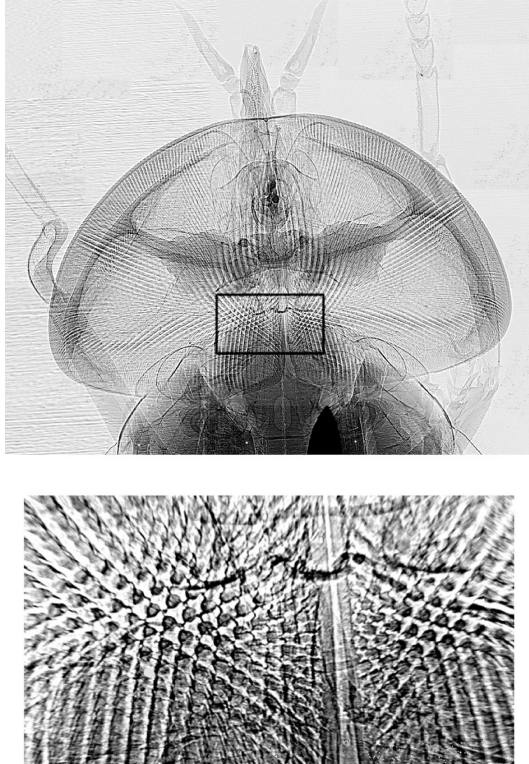


Figure 13: Another example (Ref. 13) of coherence-based radiology: the head of an insect.

This was indeed the objective of a major effort in the early history of synchrotron light. As we already discussed, progress along this direction

saturated in the mid-1980's.

The attention thus shifted to the geometric factors. The source size and the divergence were greatly improved by closer control of the electron beam around the ring and by more advanced storage ring designs. This resulted in very spectacular increases in the brightness, by orders and orders of magnitude.

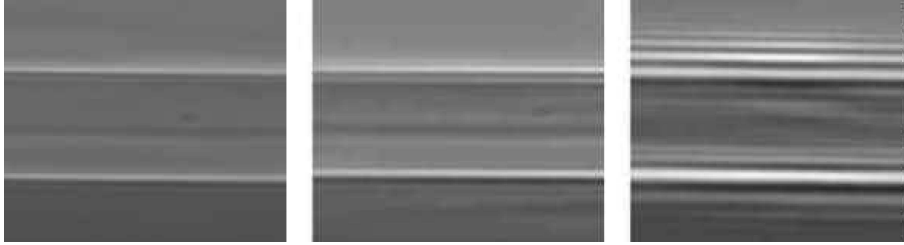


Figure 14: By changing the geometry in coherence-based radiology, one can move from the edge-refraction-enhancement regime (left) to the edge-diffraction-enhancement regime (right). The images show the two edge between different parts of an optical fiber (Ref. 7).

We have seen, however, that this progress cannot go on forever: the improvement of the source geometry cannot overcome the diffraction limit set by the wavelength. The actual sources are getting closer and closer to the diffraction limit. However, substantial improvements in the source geometry and brightness are still possible for hard-X-rays, since the diffraction limit is still far away at small wavelengths. On the contrary, limited improvements or no improvement at all are possible at longer wavelengths.

This sobering assessment changes somewhat if one consider not the *average* brightness, but the *peak* brightness of very short pulses. Spectacular improvements can in fact be achieved by enhancing the peak flux.

This is possible using a laser mechanism. As it is well known, a laser is a source based on the light emission mechanism called “stimulated” emission. Such a mechanism produces the “optical amplification” characteristic of a laser. The amplification is almost always enhanced by an “optical cavity” formed by two mirrors.

A synchrotron source is not a laser since it is not based on stimulated emission. In fact, its electrons emit photons independently from each other through “spontaneous” emission. In spite of this and thanks to relativity, we have seen that the source reaches collimation and brightness levels comparable to a laser. In other words, it is a “laser-like” source, but not a laser.

True laser action by electrons in an accelerator can be achieved with a different approach. Under the right conditions, an electron packet interacting with a wiggler can produce substantial stimulated emission and therefore optical amplification[9]. Laser action of this type was accomplished many years ago. Since the active medium is formed by electrons in vacuum, a device of this kind is called a free-electron laser (FEL)[9].

The FEL technology is primarily used for the emission of infrared light rather than for X-rays. This is due to two facts: first, the optical amplification decreases with the wavelength. Second, no mirrors and therefore no optical cavities exist for X-rays.

The only way to build an X-ray FEL is to increase the optical amplification so much that the optical cavity is no longer necessary. This is the basic philosophy of the so-called SASE (Self-Amplified Spontaneous Emission) FEL's[10].

Not tested and even controversial for a few years, the SASE concept recently became - literally - a very bright reality. Test experiments with the TESLA facility in Hamburg (HASYLAB-DESY)[11] demonstrated laser action in excellent agreement with the SASE theory. Positive results were also obtained at Argonne at higher wavelengths[12]. This may open the way to a whole new generation of sources with peak brightness more than ten orders of magnitude higher than existing sources.

Note, however, that the future X-ray FEL's will not replace storage ring. Their working mechanism is in fact only valid for short pulses of extremely high brightness. Such sources will thus be very useful for nonlinear phenomena and for other applications that require ultrabright short pulses. For other X-ray techniques, synchrotrons will continue to play the key role.

In a few years, pulsed X-ray FEL's will work in parallel to very advanced synchrotron sources at the service of science and technology. Together, they will constitute an unprecedented arsenal for a wide variety of research and technical fields, ranging from many branches of science to medicine and to industrial fabrication. We can thus conclude our short review by *coherently* saying that the future of this field is *brighter* than ever.

Work supported by the Swiss National Science Foundation and by the  
Ecole Polytechnique Fédérale de Lausanne

## References

- [1] G. Margaritondo, J. Synchrotron Radiation **2**, 148 (1995).

- [2] For a full discussion of synchrotron light, see: G. Margaritondo: “Introduction to Synchrotron Radiation” (Oxford University Press, New York 1988); Riv. Nuovo Cimento **18**, 1 (1995), and the references therein.
- [3] G. Margaritondo, Nuovo Cimento **20 D**, 1083 (1998).
- [4] F. E. Carroll, J. W. Waters, R. H. Traeger, M. H. Mendenhall, W. Clark and C. Brau, Proc. SPIE Conference on Free-Electron Laser Challenges, ISPIE **3614**, 139 (1999), and the references therein.
- [5] F. Arfelli, M. Assante, V. Bonvicini, A. Bravin, G. Cantatore, E. Castelli, L. dalla Palma, M. de Michiel, R. Longo, A. Olivo, S. Pani, D. Pontoni, P. Poropat, M. Prest, A. Rashevsky, G. Tromba, A. Vacchi, E. Vallazza, F. Zanconati, Phys. Med. Biol. **43**, 2845(1998); A. Snigirev, I. Snigireva, V. Kohn, S. Kuznetsov and I. Schelokov, Rev. Sci. Instrum. **66**, 5486 (1995); A. Snigirev, I. Snigireva, A. Suvorov, M. Kocsis and V. Kohn, ESRF Newsletters **24**, 23 (1995); D. Chapman, W. Thomlinson, R. E. Johnsson, D. Washburn, E. Pisano, N. Gmür, Z. Zhong, R. Menk, F. Arfelli and D. Sayers, Phys. Med. Biol. **42**, 2015 (1997); A. Pogany, D. Gao and S. W. Wilkins, Rev. Sci. Instrum. **68**, 2774 (1997); S. W. Wilkins, T. E. Gureyev, D. Gao, A. Pogany and A. W. Stevenson, Nature **384**, 335 (1996); K. A. Nugent, T. E. Gureyev, D. F. Cookson, D. Paganin and Z. Barnea, Phys. Rev. Lett. **77**, 2961 (1996); Y. Kagoshima, Y. Tsusaka, K. Yokoyama, K. Takai, S. Takeda, J. Matsui, Jpn. J. Appl. Phys. **38**, L470 (1999); A. Momose, Medical Imaging Technology **17**, 18 (1999); S. Di Fonzo, W. Jark, G. Soullie, A. Cedola, S. Lagomarsino, P. Cloetens, C. Riekel, J. Synchrotron Radiation **5**, 376 (1998).
- [6] G. Margaritondo and G. Tromba, J. Appl. Phys. **85**, 3406 (1999); G. Margaritondo, G. Tromba, Y. Hwu and M. Grioni, Phys. Low. Dim. Struct. **11/12**, 39 (1998); Y. Hwu, B. Lai, D. C. Mancini, J. H. Je, D. Y. Noh, M. Bertolo, G. Tromba and G. Margaritondo, Appl. Phys. Letters **75**, 2377 (1999).
- [7] Y. Hwu, H. H. Hsieh, M. J. Lu, W. L. Tsai, H. M. Lin, W. C. Goh, B. Lai, J. H. Je, C. K. Kim, D. Y. Noh, H. S. Youn, G. Tromba and G. Margaritondo, J. Appl. Phys. **86**, 4613 (1999).
- [8] Kyu-Ho Lee, Y. Hwu, Jung-Ho Je, Wen-Li Chai, Hee-Joung Kim, Je-Kyung Seong, Seung-Won Yi, Hyung-Sik Ryo and G. Margaritondo, unpublished.

- [9] G. Margaritondo: *Introduction to Synchrotron Radiation* (Oxford, New York, 1988).
- [10] R. Bonifacio, C. Pellegrini and L. Narducci, *Opt. Commun.* **50**, 6 (1985); “A *VUV Free Electron Laser at the TESLA Test Facility at DESY – Conceptual Design Report*” TESLA-FEL 95-03 (DESY Print, Hamburg 1995); Y. S. Derbenev, A. M. Kondratenko, and E. L. Saldin, *Nucl. Instrum. Methods* **193**, 415 (1982);
- [11] J. Andruszkow *et al.*, *Phys. Rev. Lett.* (in press).
- [12] S. V. Milton, E. Gluskin, S. G. Biedron, R. J. Dejus, P. K. Den Hartog, J. N. Galayda, K.-J. Kim, J. W. Lewellen, E. R. Moog, V. Sajaev, N. S. Sereno, G. Travish, N. A. Vinokurov, N. D. Arnold, C. Benson, W. Berg, J. A. Biggs, M. Borland, J. A. Carwardine, Y.-C. Chae, G. Decker, B. N. Deriy, M. J. Erdmann, H. Friedsam, C. Gold, A. E. Grelick, M. W. Hahne, K. C. Harkay, Z. Huang, E. S. Lessner, R. M. Lill, A. H. Lumpkin, O. A. Makarov, G. M. Markovich, D. Meyer, A. Nassiri, J. R. Noonan, S. J. Pasky, G. Pile, T. L. Smith, R. Soliday, B. J. Tieman, E. M. Trakhtenberg, G. F. Trento, I. B. Vasserman, D. R. Walters, X. J. Wang, G. Wiemerslage, S. Xu, and B.-X. Yang, *Phys. Rev. Lett.* **85**, 988 (2000).
- [13] Y. Hwu, J. H. Je *et al.*, unpublished data.